Supplementary methods

Mechanical itch behavior

Touch evoked scratching was tested as previously reported (Pan *et al.*, 2019). The fur behind the ears (pale yellow) was shaved 5 days before testing. Mice were habituated for 1 hour for 2 consecutive days in behavioral testing apparatus. Mice then received 10 separate mechanical stimuli with a 0.7 mN von-Frey filament on the skin behind the ears. The scratching response of hind paw toward the poking site was considered as a positive response. The percentile of positive responses in 10 stimuli was determined as an acute mechanical itch score.

Von Frey Testing for Mechanical threshold

Mice were habituated in boxes (14 × 18 × 12 cm) placed on an elevated metal mesh floor for at least 2 days before testing. All the tests were conducted blindly. Mice were stimulated on their hind paws with a series of von Frey filaments with logarithmically increasing stiffness (0.16-2.00 g, Stoelting). The filaments were presented perpendicularly to the central plantar surface of a hind paw (Chen *et al.*, 2018). The paw withdrawal threshold was determined by Dixon's up-down method.

Supplementary Figures

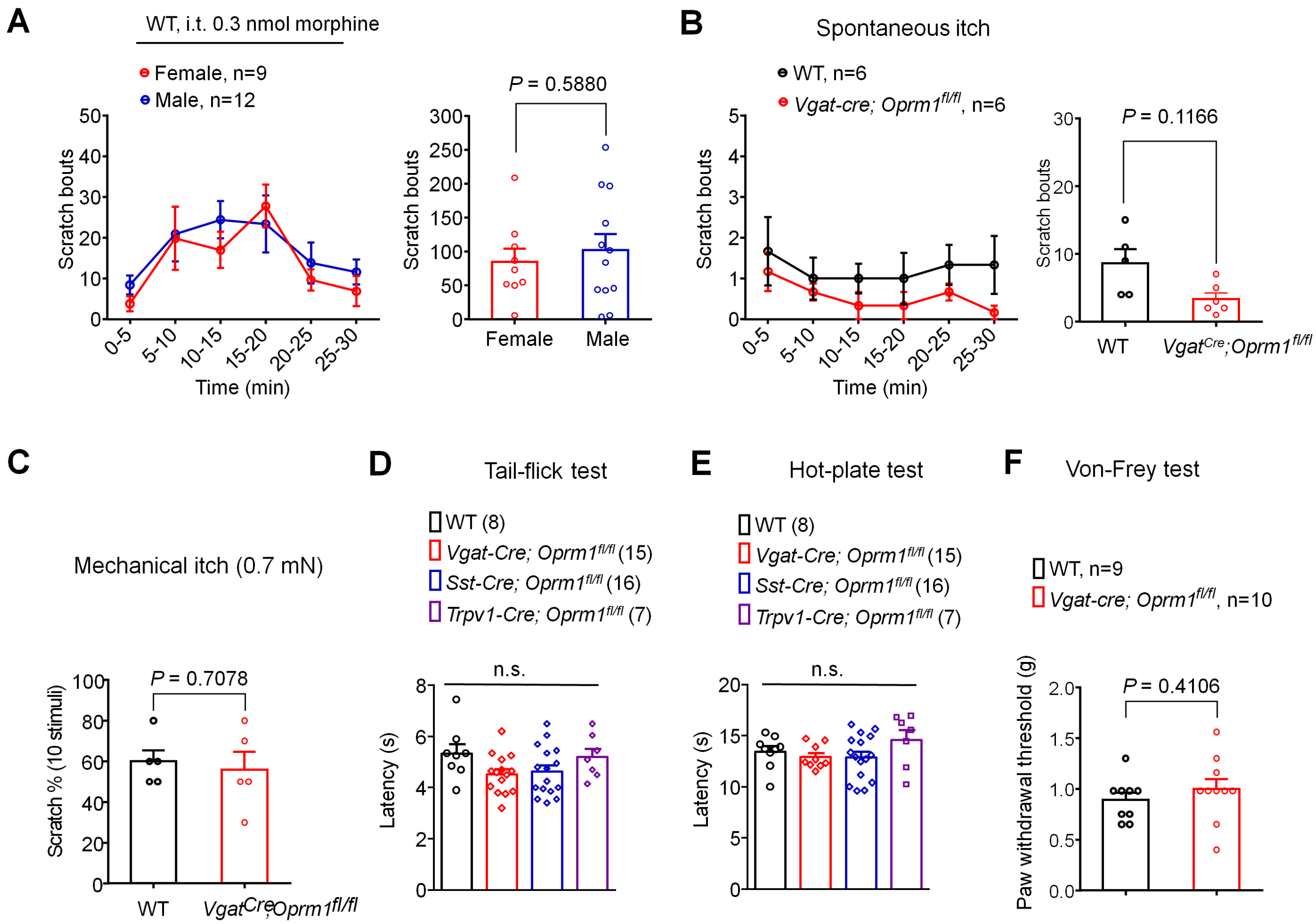

Figure S1. Basal response in pain and itch in wild-type and transgenic mice

(A) Intrathecal morphine induced itch in male and female mice. *P* = 0.5880, two-tailed Student's t-test. **(B)** Spontaneous itch in WT and *Vgat-Cre; Oprm1$^{fl/fl}$* mice within 30 min. *P* = 0.1166, two-tailed Student's t-test. **(C)** Mechanical itch evoked by 0.7 mN von-Frey filament in WT and *Vgat-Cre; Oprm1$^{fl/fl}$* mice. *P* = 0.7078, two-tailed Student's t-test. **(D-E)** Tail-flick (D) and hot-plate (E) tests in WT, *Vgat-Cre; Oprm1$^{fl/fl}$*, *Sst-Cre; Oprm1$^{fl/fl}$*, *Trpv1-Cre; Oprm1$^{fl/fl}$* mice. n.s., no significance, one-way ANOVA. **(F)** Paw withdrawal threshold in WT and *Vgat-Cre; Oprm1$^{fl/fl}$* mice. *P* = 0.4106, two-tailed Student's t-test. Data are Mean ± SEM.

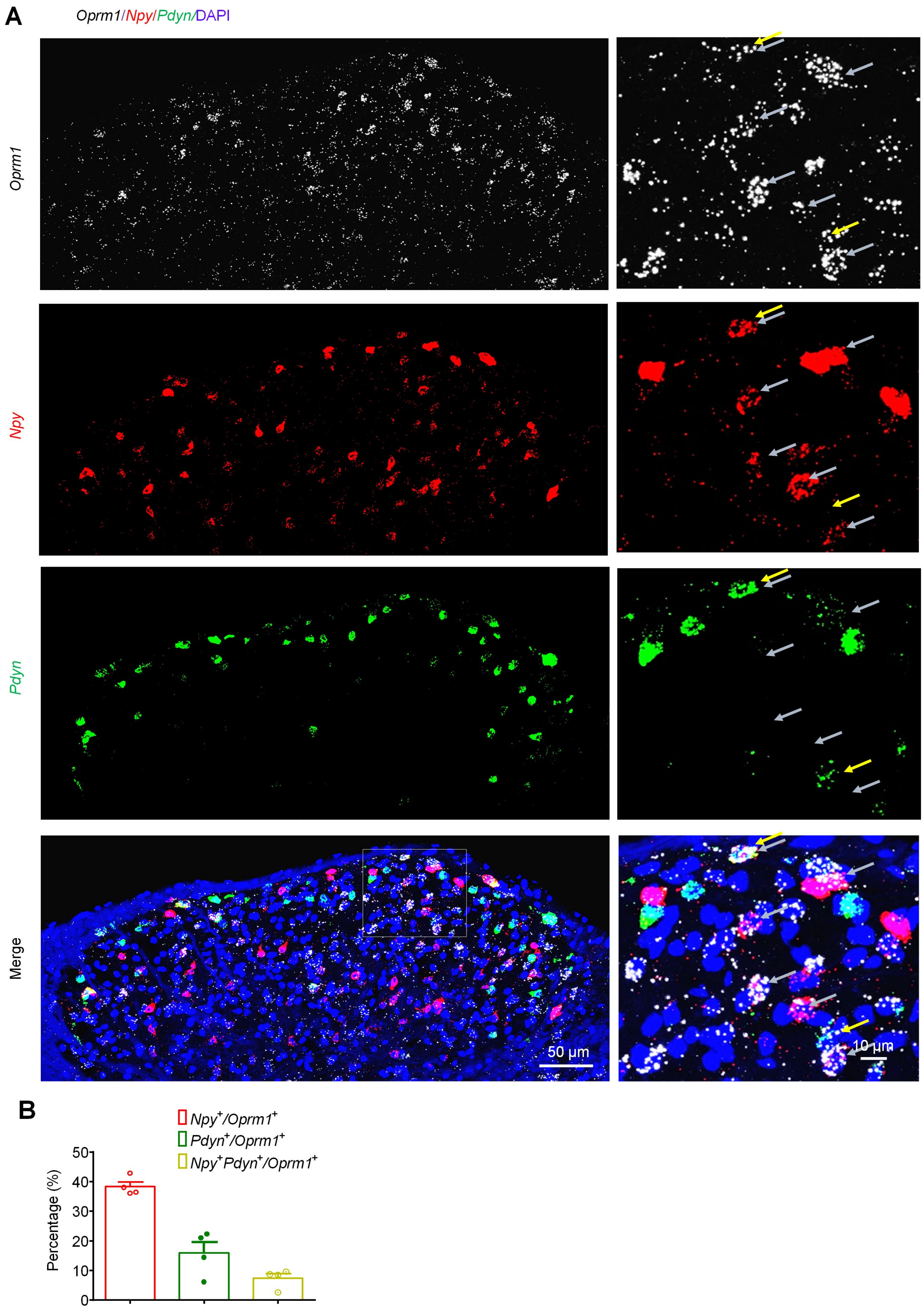

Figure S2. ***Oprm1*** **expression in** ***Npy***$^{+}$ **and** ***Pdyn***$^{+}$ **interneurons in the spinal cord dorsal horn (SDH). (A)** In situ hybridization (RNAscope) images showing mRNA expression for *Oprm1* (white), *Npy* (red) and *Pdyn* (encoding Pro-Dynorphin, green) in WT mouse SDH. Yellow and gray arrows indicate *Oprm1* co-localization with *Pdyn* or *Npy*, respectively. Scale bar, 50 μm (left) 10 μm (right). **(B)** The percentage of co-expression of *Oprm1* with *Npy* and *Pydn* in SDH neurons. Eight spinal cord sections from 4 mice were analyzed.

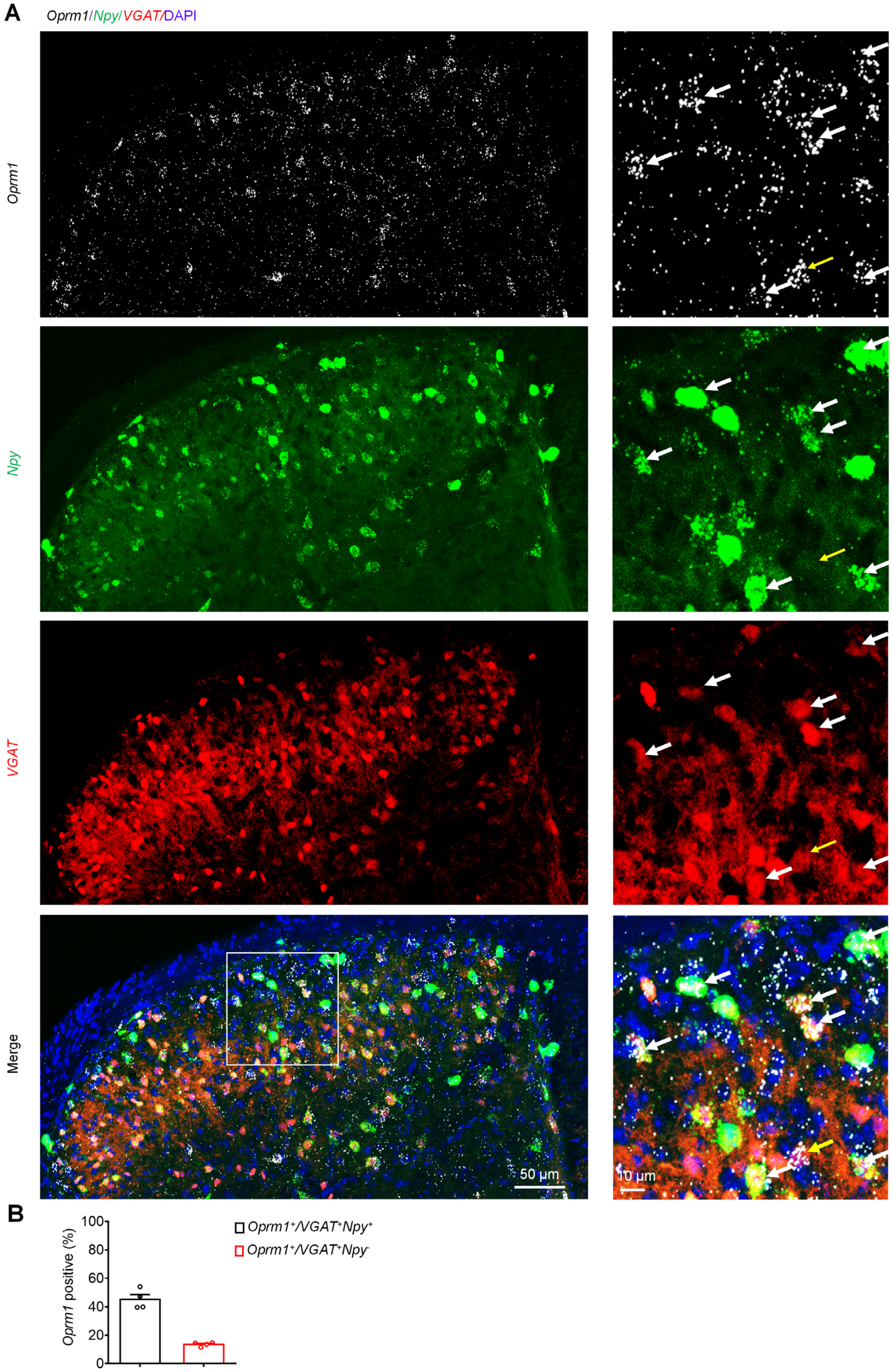

Figure S3. *Oprm1* expression in *Npy*$^+$ inhibitory interneurons in the spinal cord dorsal horn (SDH).

(A) In situ hybridization (RNAscope) images showing mRNA expression for *Oprm1* (white), *Npy* (green) and Vgat^{tdTomato} (red) in the SDH from Vgat-cre;Ai9 mouse. White arrows indicate *Oprm1* in *Npy*$^+$ inhibitory neurons and yellow arrow indicate *Oprm1* in *Npy*$^-$ inhibitory neurons. Scale bars, 50 µm (left) and 10 µm (right). **(B)** The percentage of *Oprm1* in *Npy*$^+$ inhibitory neurons and *Npy*$^-$ inhibitory neurons. Eight spinal cord sections from 4 mice were analyzed.

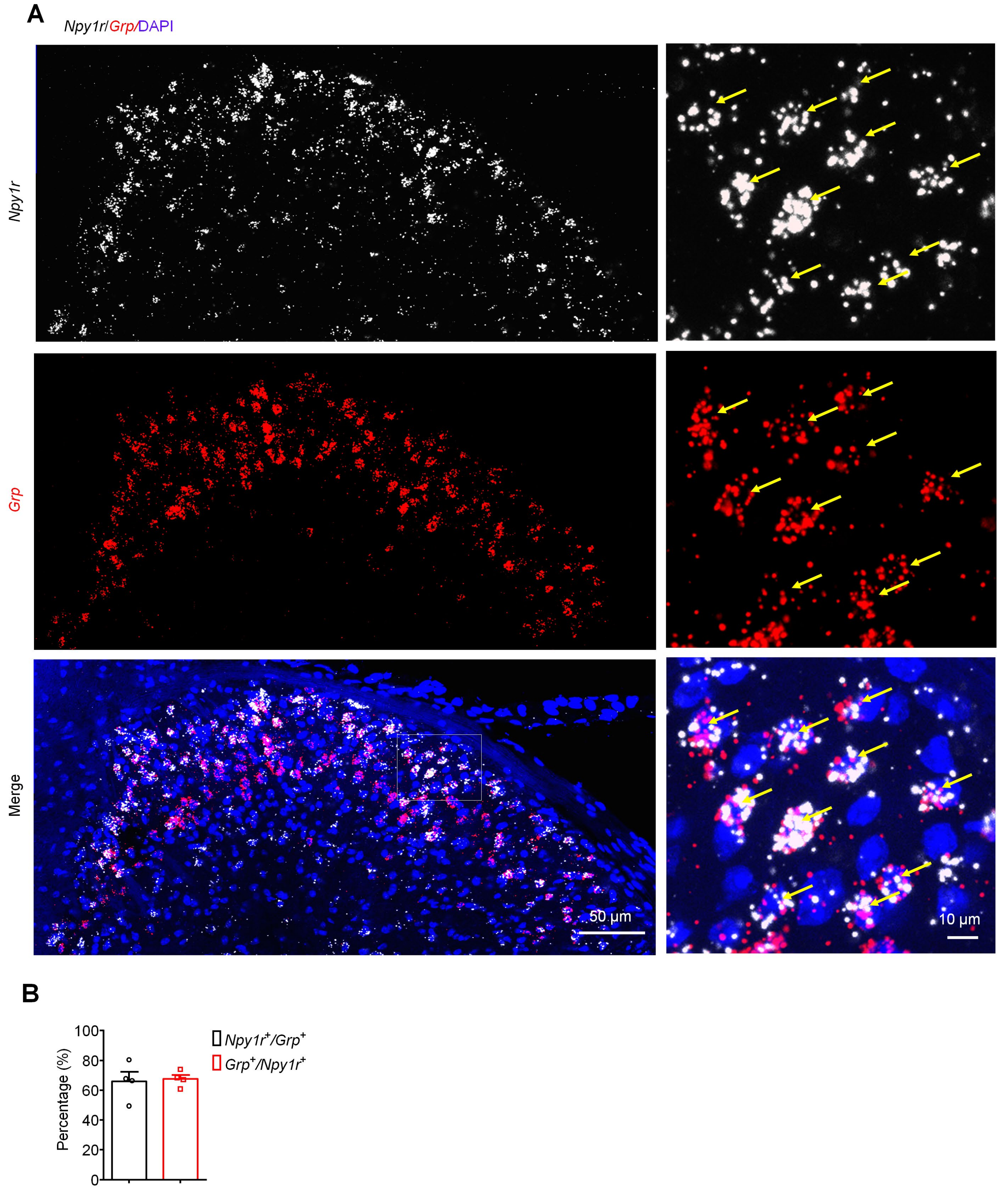

Figure S4. Co-expression of *Grp* and *Npy1r* in the SDH.

(A) In situ hybridization (RNAscope) images showing the co-expression of *Npy1r* (white) and *Grp* (red) in WT mouse SDH. Yellow arrows show *Npy1r* double labelling with *Grp*. Scale bars, 50 μm (left) and 10 μm (right). **(B)** The percentage of co-expression of *Npy1r* with *Grp* in SDH neurons. Eight spinal cord sections from 4 mice were analyzed. Data are Mean ± SEM.

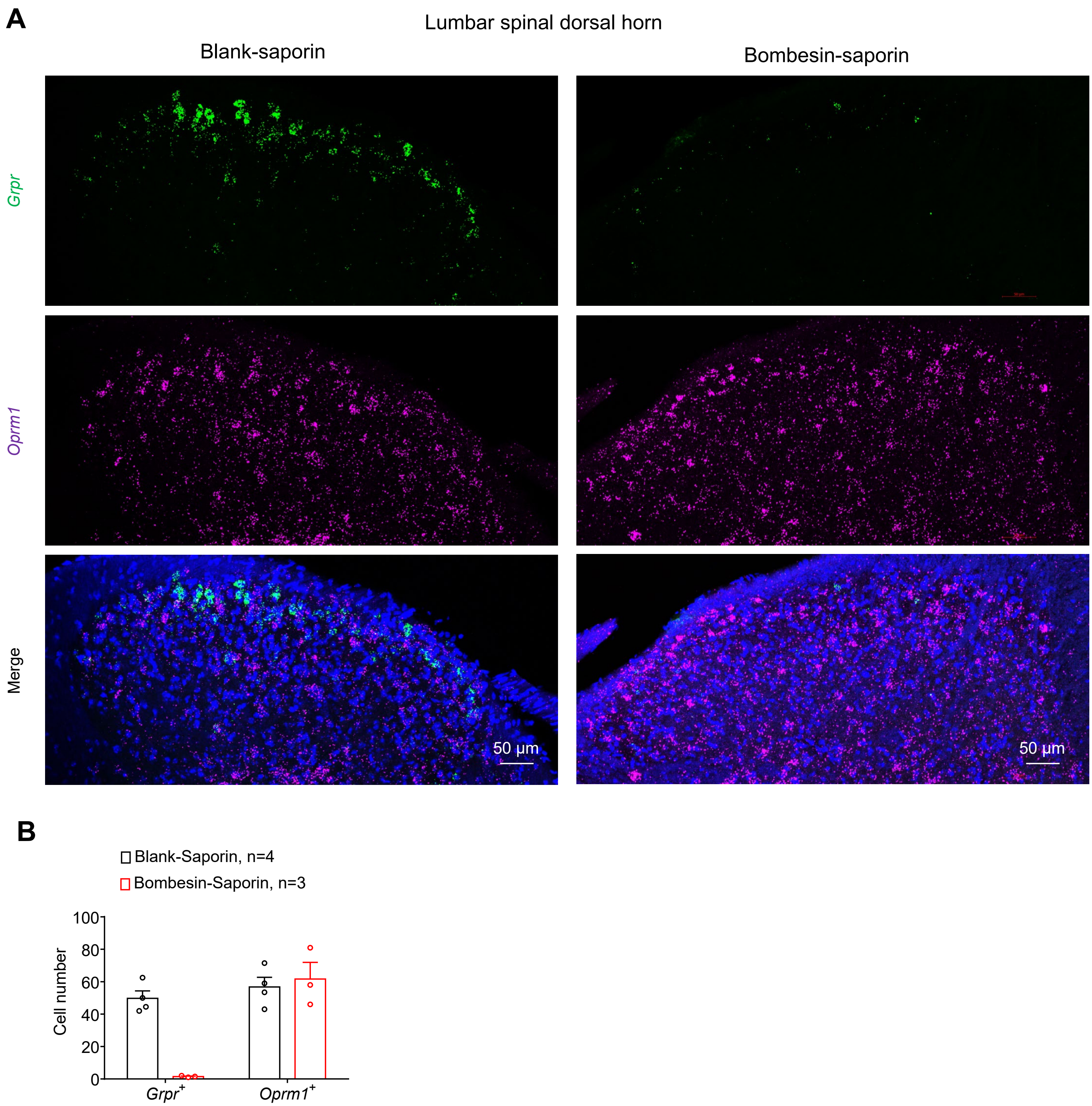

Figure S5. GRPR ablation in the lumbar spinal dorsal horn.

(A) In situ hybridization (RNAscope) images showing the expression of *Grpr* (green) and *Oprm1* (purple) in WT mouse lumbar SDH treated with 400 ng Blank-saporin (left) and Bombesin-saporin (right). Scale bars, 50 μm (left) and 10 μm (right). **(B)** Number of positive cells for *Grpr and Oprm1* in SDH. Six to eight spinal cord sections from 3-4 mice were analyzed. Data are Mean ± SEM.

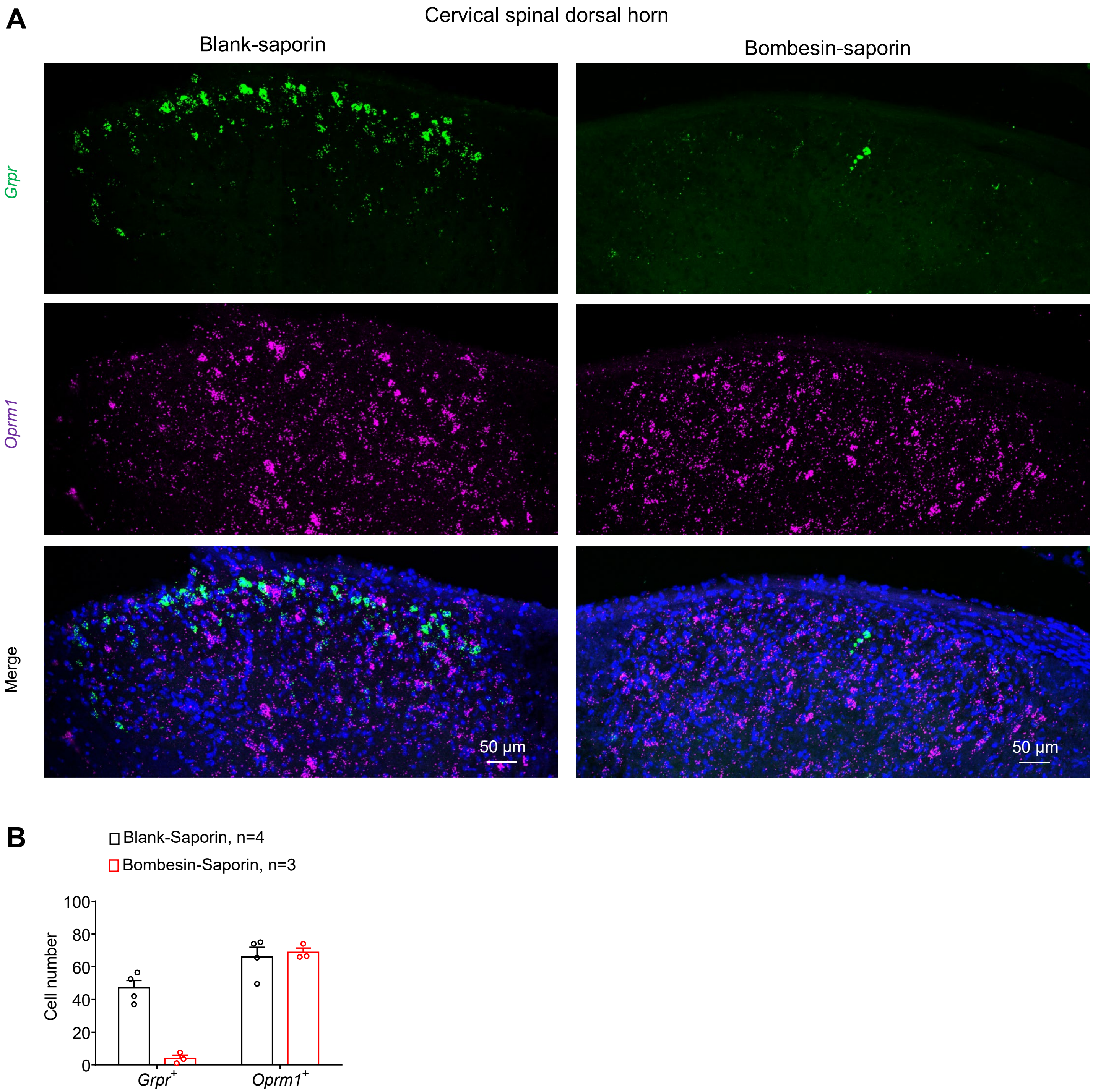

Figure S6. GRPR ablation in the cervical spinal dorsal horn.

(A) In situ hybridization (RNAscope) images showing the expression of *Grpr* (green) and *Oprm1* (purple) in WT mouse cervical SDH treated with 400 ng Blank-saporin (left) and Bombesin-saporin (right). Scale bars, 50 μm (left) and 10 μm (right). **(B)** Number of positive cells for *Grpr and Oprm1* in SDH. Six to eight spinal cord sections from 3-4 mice were analyzed. Data are Mean ± SEM.

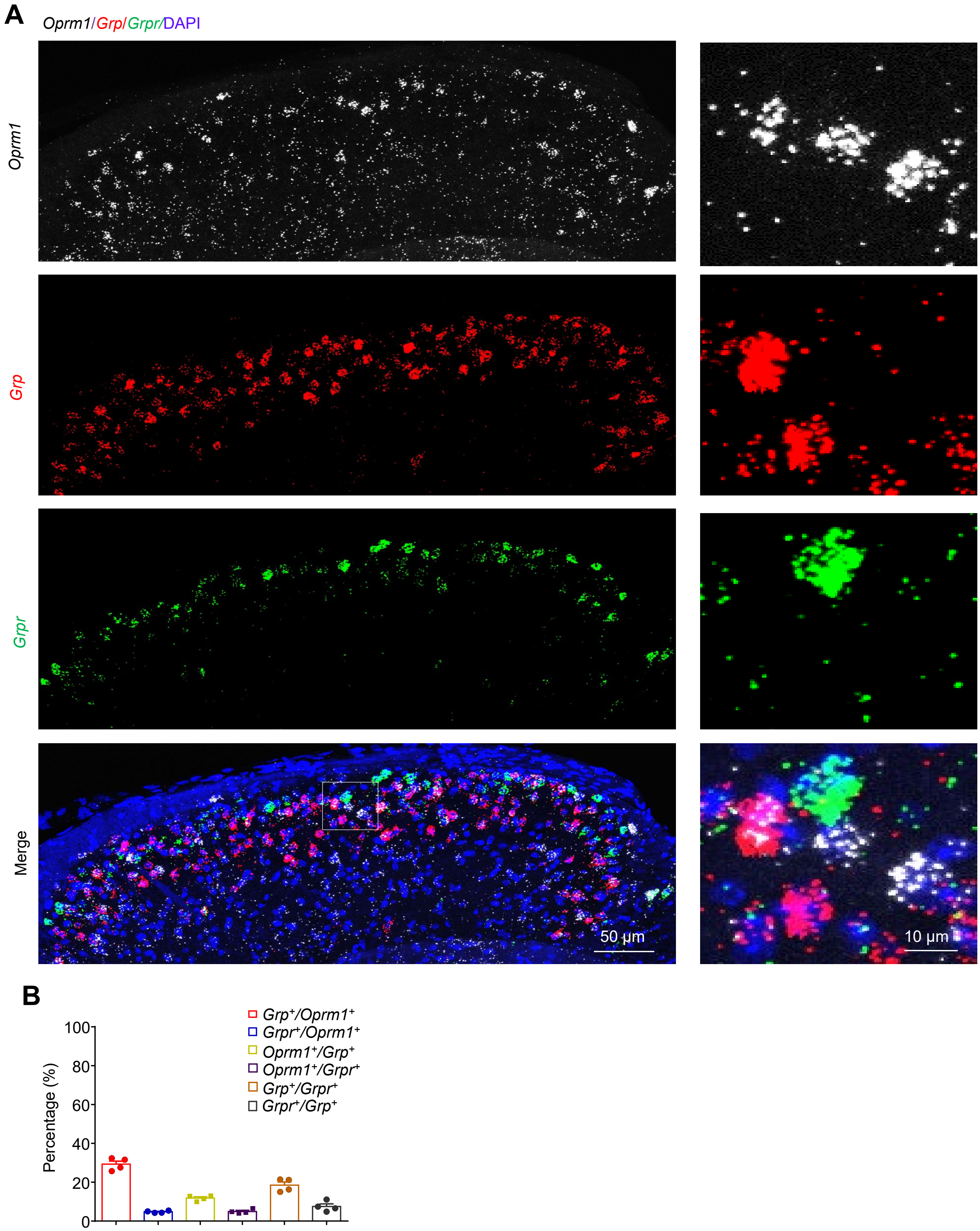

Figure S7. Limited co-expression of *Oprm1* with *Grpr* in SDH.

(A) In situ hybridization (RNAscope) images showing mRNA expression of *Oprm1* (white), *Grp* (red), and *Grpr* in WT mouse SDH. Scale bars, 50 μm (left) and 10 μm (right). **(B)** The percentage of co-expression of *Oprm1*$^{+}$, Grp^{+}, Grpr^{+} neurons in mouse SDH. Eight spinal cord sections from 4 mice were analyzed. Data are Mean ± SEM.

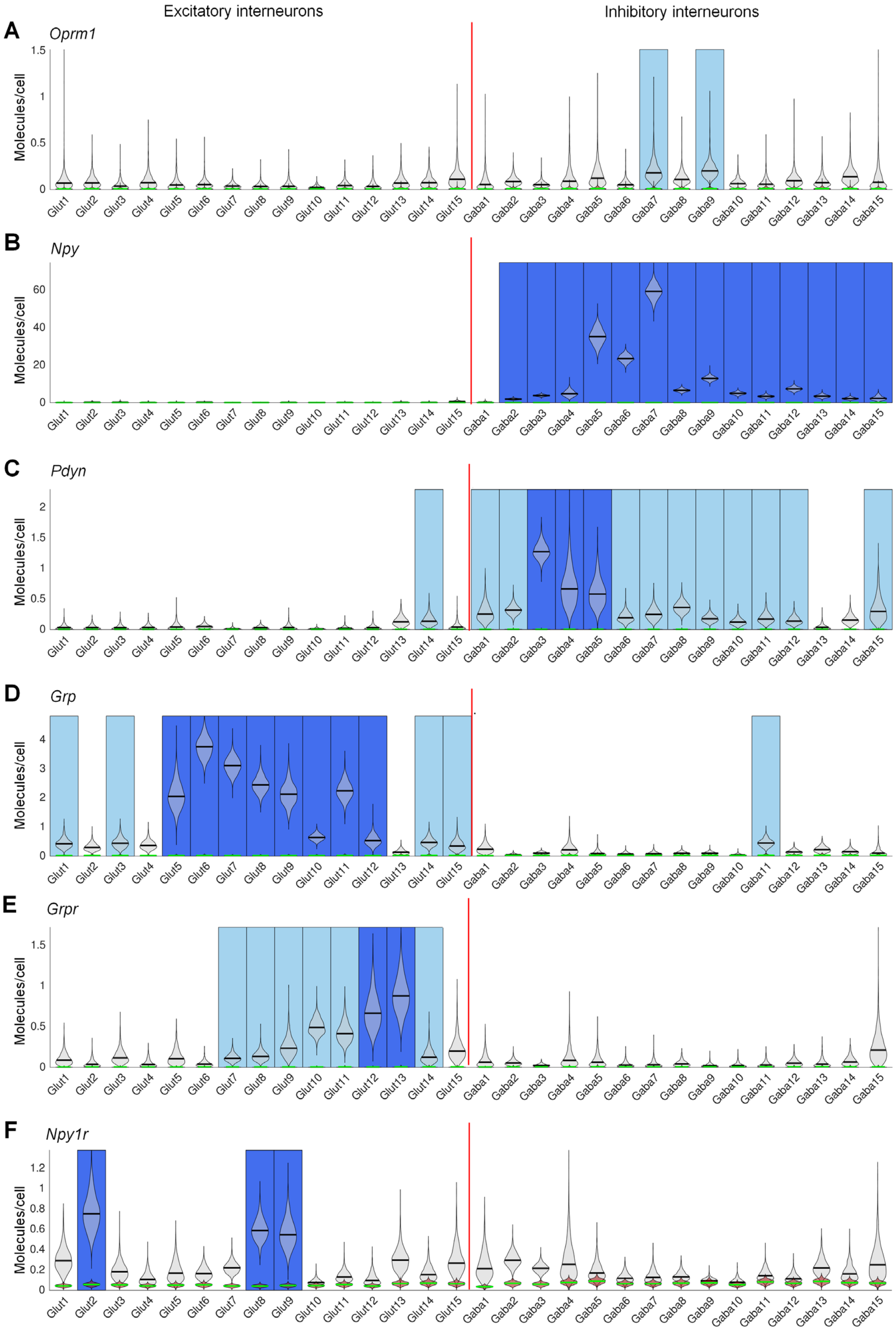

Figure S8. Single-cell RNA sequencing database showing gene expression in mouse SDH.

Expression patterns of *Oprm1* (A), *Npy* (B), *Pdyn* (C), *Grp* (D), *Grpr* (E), and *Npy1r* (F) in the mouse spinal cord revealed by single cell RNA sequencing (Haring *et al.*, Nat. Neurosci. 2018). Note, *Oprm1* (A) is expressed in both excitatory and inhibitory interneurons, with the highest expression of *Oprm1* in Baba 7 and 9 populations, which also co-express *Npy* (B). The highest expression of *Npy1r* is seen in the Glut 2, 8 and 9 populations, and *Npy1r* in Glut 8 and 9 populations co-express *Grp*.

Table S1: Number of animals used in this study

Experiment	Figures	Sample size	Number of groups	Sample number	Sex	Age (Months)	Number of animals
Figure 1	Figure 1A	n = 5-9 mice	6	38	10 male, 28 female	2-4	38 WT mice
	Figure 1B	n = 10-12 mice	2	22	9 male, 13 female	2-4	22 WT mice
	Figure 1C,D	n = 9-12 mice	2	21	11 male, 10 female	2-4	9 WT mice, 12 *Vgat-Cre; Oprm1*$^{fl/fl}$ mice
	Figure 1E,F	n = 9-11 mice	2	18	16 male, 4 female	2-4	11 WT mice, 9 *Sst-Cre; Oprm1*$^{fl/fl}$ mice
	Figure 1G	n = 5 mice	5	25	18 male, 7 female	2-4	25 WT mice
	Figure 1H	n = 6-7 mice	2	13	8 male, 5 female	2-4	6 WT mice, 7 *Vgat-Cre; Oprm1*$^{fl/fl}$ mice
Figure 2	Figure 2A	n = 7-9 mice	2	16	5 male,9 female	2-4	16 WT mice
	Figure 2B	n = 6-8 mice	2	14	8 male, 6 female	2-4	14 WT mice
	Figure 2C,D	n = 10-13 mice	2	23	10 male, 13 female	2-4	10 WT mice, 13 *Trpv1-Cre; Oprm1*$^{fl/fl}$ mice
	Figure 2E	n =10 mice	2	20	15 male, 5 female	2-4	20 WT mice
	Figure 2F	n =5 mice	2	10	7 male, 3 female	2-4	5 WT mice, 5 *Vgat-Cre; Oprm1*$^{fl/fl}$ mice
Figure 3	Figure 3A,B	n = 7-11 mice	4	36	22 male, 14 female	2-4	10 WT mice, 7 *Vgat-Cre; Oprm1*$^{fl/fl}$ mice, 8 *Sst-Cre; Oprm1*$^{fl/fl}$ mice, 11 *Trpv1-Cre; Oprm1*$^{fl/fl}$ mice
	Figure 3C,D	N = 5-10 mice	6 (2 were same with Figure 3A,B)	11	13 male, 9 female	2-4	11 WT mice, 11 *Vgat-Cre; Oprm1*$^{fl/fl}$ mice,
Figure 4	Figure 4A,B	n = 4 mice	1	4	4 male	2-4	4 *Vgat-Cre; tdTomato* mice
Figure 5	Figure 5A	n = 19 neurons from 5 mice	1	19	3 male, 2 female	1-2	5 *Vgat-Cre; tdTomato* mice
	Figure 5B,C	n = 15 neurons from 5 mice	1	15	3 male, 2 female	1-2	5 *Vgat-Cre; tdTomato* mice
	Figure 5D,E	n = 9-14 neurons from 5-6 mice	2	10,15	7 male, 4 female	1-2	11 *Vgat-Cre;* Ai32 mice
Figure 6	Figure 6A	n = 6-10 mice	2	16	6 male, 10 female	2-4	16 WT mice
	Figure 6B	n = 6-7 mice	2	13	9 male, 4 female	2-4	13 WT mice
	Figure 6C	n = 6-7 mice	2	13	9 male, 4 female	2-4	13 WT mice
	Figure 6D	n = 7 mice	2	14	9 male, 5 female	2-4	7 WT mice, 7 *Vgat-Cre; Oprm1*$^{fl/fl}$ mice
Figure 7	Figure 7A,B	n = 8-9 mice	2	17	8 male, 9 female	2-4	8 WT mice, 9 *Vgat-Cre; Oprm1*$^{fl/fl}$ mice
	Figure 7C	n = 8-9 mice	2	17	11 male, 6 female	2-4	9 WT mice, 8 *Vgat-Cre; Oprm1*$^{fl/fl}$ mice
	Figure 7D	n = 5-6 mice	2	11	7 male, 4 female	2-4	5 WT mice, 6 *Vgat-Cre; Oprm1*$^{fl/fl}$ mice
	Figure 7E	n = 7-8 mice	2	15	11 male, 4 female	2-4	15 WT mice
	Figure 7F	n = 8-9 mice	2	17	10 male, 7 female	2-4	17 WT mice
Figure 8	Figure 8A	n = 6-10 mice	3	22	4 male, 18 female	2-4	22 WT mice
	Figure 8B	n = 9 mice	2	18	6 male, 12 female	2-4	18 WT mice
	Figure 8C	n = 8 mice	3	24	12 male, 12 female	2-4	24 NOD. CB-17-Prkdc^{scid} mice
	Figure 8D	n = 13-14 mice	2	27	13 male, 14 female	2-4	27 NOD. CB-17-Prkdc^{scid} mice
Figure S1	Figure S1A	n = 9-12 mice	2 (same mice from Figure 1)	21	9 male, 12 female	2-4	21 WT mice
	Figure S1B	n = 6 mice	2	12	6 male, 6 female	2-4	6 WT mice, 6 *Vgat-Cre; Oprm1*$^{fl/fl}$ mice
	Figure S1C	n = 5 mice	2	10	10 male	2-4	5 WT mice, 5 *Vgat-Cre; Oprm1*$^{fl/fl}$ mice
	Figure S1D,E	n = 7-16 mice	4(same mice from Figure 3)	33	25 male, 21 female	2-4	8 WT mice, 15 *Vgat-Cre; Oprm1*$^{fl/fl}$ mice, 16 *Sst-Cre; Oprm1*$^{fl/fl}$ mice, 7*Trpv1-Cre; Oprm1*$^{fl/fl}$ mice
	Figure S1F	n = 9-10 mice	2	19	10 male, 9 female	2-4	9 WT mice, 10 *Vgat-Cre; Oprm1*$^{fl/fl}$ mice
Figure S2	Figure S2	n = 4 mice	1	4	4 male	2-4	4 WT mice
Figure S3	Figure S3	n = 4 mice	1	4	4 male	2-4	4 *Vgat-Cre; tdTomato* mice
Figure S4	Figure S4	n = 4 mice	1	4	4 male	2-4	4 WT mice
Figure S5	Figure S5	n = 3-4 mice	2	4	4 male	2-4	7 WT mice
Figure S6	Figure S6	n = 3-4 mice	2 (same mice from Figure S5)	7	3 male, 4 female	2-4	7 WT mice
Figure S7	Figure S7	n = 4 mice	1	4	4 male	2-4	4 WT mice
Total number of mice					309 male, 249 female		558 mice

Reference List

Pan H, Fatima M, Li A, Lee H, Cai W, Horwitz L, *et al.* Identification of a Spinal Circuit for Mechanical and Persistent Spontaneous Itch. Neuron 2019; 103(6): 1135-49 e6.

Chen G, Luo X, Qadri MY, Berta T, Ji RR. Sex-Dependent Glial Signaling in Pathological Pain: Distinct Roles of Spinal Microglia and Astrocytes. Neurosci Bull 2018; 34(1): 98-108.

Haring M, Zeisel A, Hochgerner H, Rinwa P, Jakobsson JET, Lonnerberg P, *et al.* Neuronal atlas of the dorsal horn defines its architecture and links sensory input to transcriptional cell types. Nat Neurosci 2018; 21(6): 869-80.